

Quantum-accurate Force Fields from Machine Learning of Large Materials Data

Xiang-Guo Li, Zhi Deng, Yunxing Zuo, Chi Chen,
Shyue Ping Ong

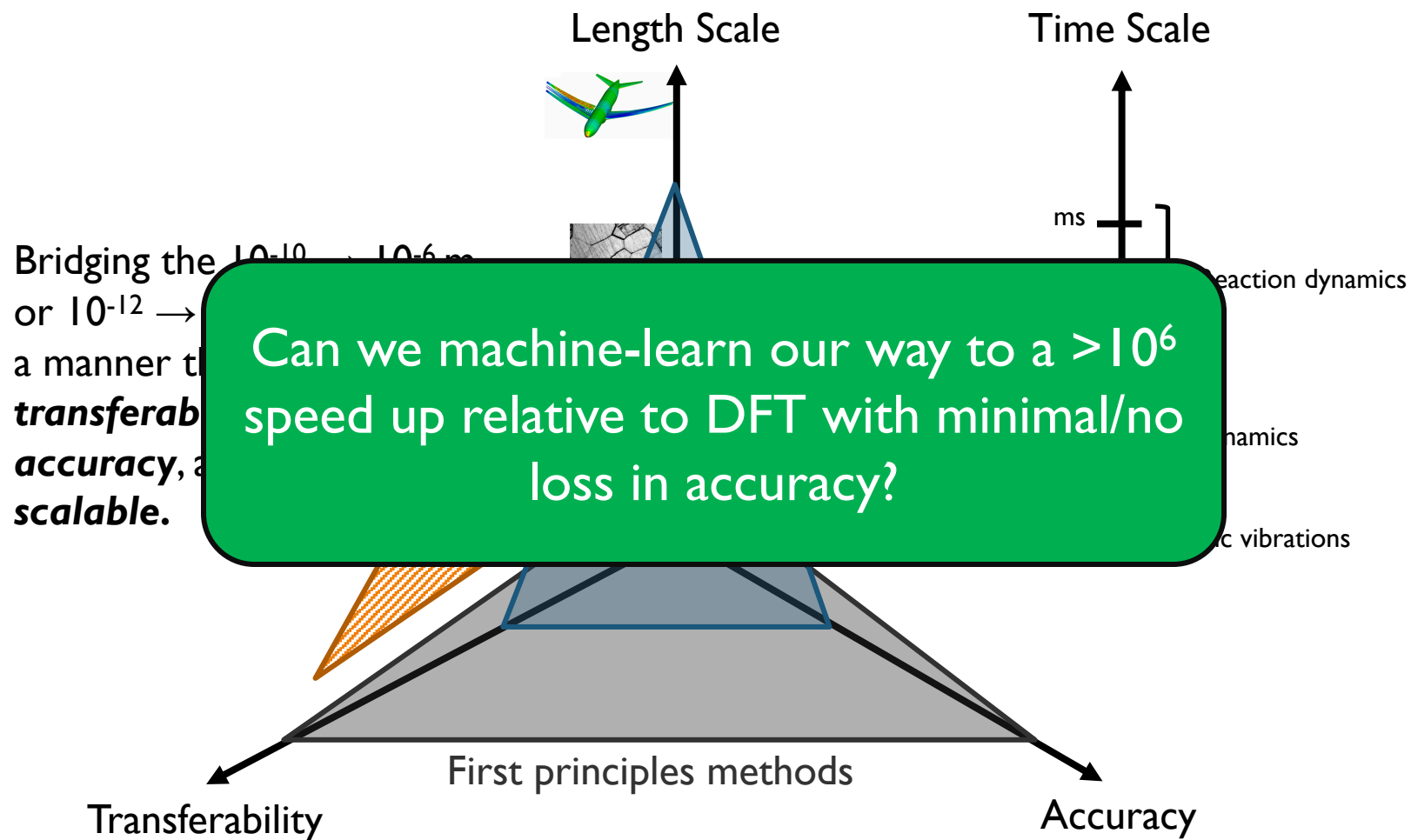
8/29/19

Albuquerque 2019

UC San Diego
Jacobs School of Engineering


materials
virtual·lab —

Scale Challenge in Computational Materials Science



General procedure

Sample a sufficiently large dataset

Describe local environment

Learn relationship between features and energy, force, etc.

Open databases



OQMD

Requirements

- Invariance to rotation,

Spectral neighbor analysis potential (SNAP)

pymatgen
FireWorks

Materials



- Symmetry functions
- Bispectrum
- Smooth overlap of atomic positions
- Fragment descriptors
- ...

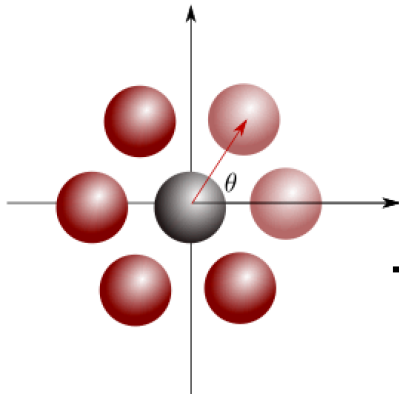
- Neural networks
-

Regression

Large regression forest

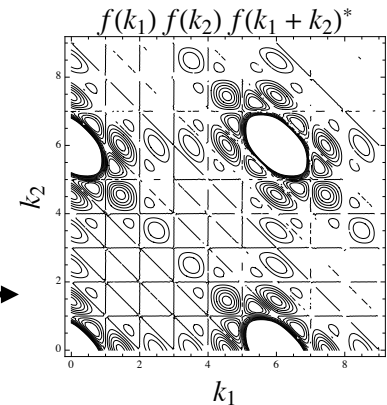
A many-body atomic environment descriptor: bispectrum coefficients

- Map neighbors into unit sphere in 4D
- Expand density in 4D spherical harmonics



$$\rho(\mathbf{r}) = \sum_{j=0, \frac{1}{2}, \dots}^{\infty} \sum_{m=-j}^j \sum_{m'=-j}^j u_{m,m'}^j U_{m,m'}^j(\theta, \phi, \theta_0)$$

Bispectrum



$$\rho_i(\mathbf{r}) = \delta(\mathbf{r}) + \sum_{r_{ii'} < R_c} f_c(r_{ii'}) w_{ii'} \delta(\mathbf{r} - \mathbf{r}_{ii'})$$

R_c^{atom} radius cutoff

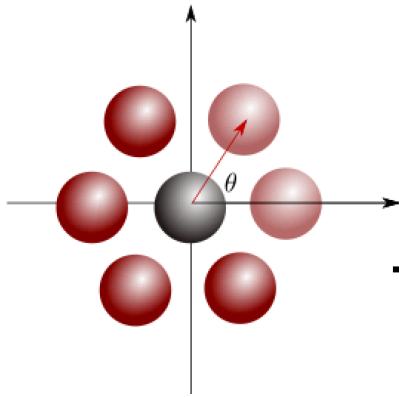
w^{atom} distinguishes species

$$B_{j_1, j_2, j} = \sum_{m_1, m'_1 = -j_1}^{j_1} \sum_{m_2, m'_2 = -j_2}^{j_2} \sum_{m, m' = -j}^j (u_{m, m'}^j)^* H_{j_2 m_2 m'_2}^{j_1 m_1 m'_1} u_{m_1, m'_1}^{j_1} u_{m_2, m'_2}^{j_2}$$

j^{max} order of Bispectrum, set to 3.

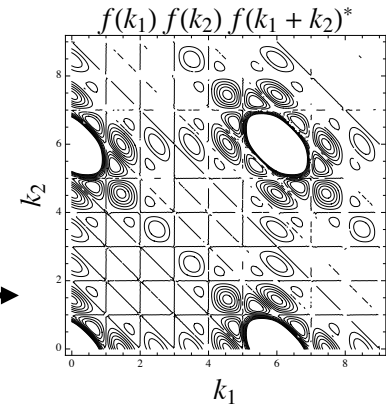
A many-body atomic environment descriptor: bispectrum coefficients

- Map neighbors into unit sphere in 4D
- Expand density in 4D spherical harmonics



$$\rho(\mathbf{r}) = \sum_{j=0, \frac{1}{2}, \dots}^{\infty} \sum_{m=-j}^j \sum_{m'=-j}^j u_{m,m'}^j U_{m,m'}^j(\theta, \phi, \theta_0)$$

Bispectrum



$$\rho_i(\mathbf{r}) = \delta(\mathbf{r}) + \sum_{r_{ii'} < R_c} f_c(r_{ii'}) w_{i'} \delta(\mathbf{r} - \mathbf{r}_{ii'})$$

$$B_{j_1, j_2, j} = \sum_{m_1, m'_1 = -j_1}^{j_1} \sum_{m_2, m'_2 = -j_2}^{j_2} \sum_{m, m' = -j}^j (u_{m, m'}^j)^* H_{j_2 m_2 m'_2}^{j m m'} u_{m_1, m'_1}^{j_1} u_{m_2, m'_2}^{j_2}$$

Spectral neighbor analysis potential (SNAP)¹

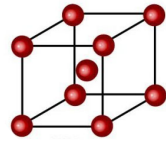
$$E_{\text{SNAP}} = \beta_0 N + \beta \cdot \sum_{i=1}^N B^i$$

$$\mathbf{F}_{\text{SNAP}}^j = -\beta \cdot \sum_{i=1}^N \frac{\partial B^i}{\partial \mathbf{r}_j}$$

$$\boldsymbol{\sigma}_{\text{SNAP}}^j = -\beta \cdot \sum_{j=1}^N \mathbf{r}_j \otimes \sum_{i=1}^N \frac{\partial B^i}{\partial \mathbf{r}_j}$$

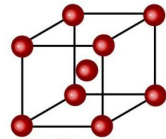
¹ Thompson et al. J. Comput. Phys. 2015, 285, 316–330

Extending the SNAP formalism



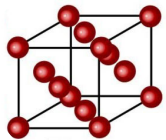
bcc
(Ta^[1], W^[2])

Sandia National Lab

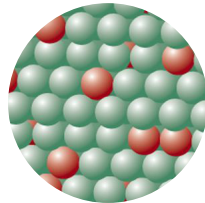


bcc
(Mo^[3])

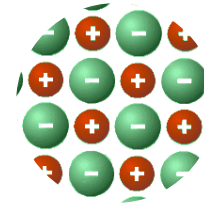
Materials Virtual Lab



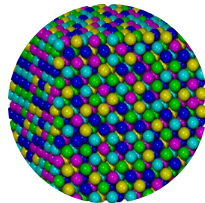
fcc
(Cu, Ni^[4])



Binary Alloys
(Ni-Mo^[4])



Ionic Crystals
(Li₃N^[5])

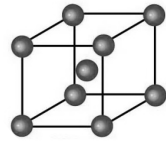


MPE Alloys
(Ta-Nb-Mo-W)

- [1] Thompson et al. *J. Comput. Phys.* **2015**, 285, 316–330.
[2] Wood et al. *arXiv preprint*. **2017**, *arXiv:1702.07042*.
[3] Chen et al. *Phys. Rev. Mater.* **2017**, 1, 043603.

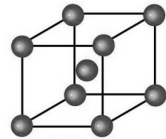
- [4] Li et al. *Phys. Rev. B.* **2018**, 98, 094104.
[5] Deng et al. *npj Comp Mat.* **2019**, 5, 75

Extending the SNAP formalism



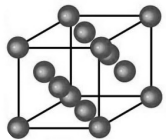
bcc
(Ta^[1], W^[2])

Sandia National Lab

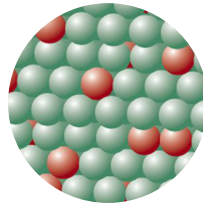


bcc
(Mo^[3])

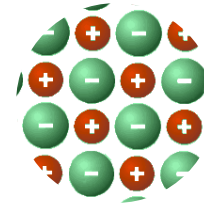
Materials Virtual Lab



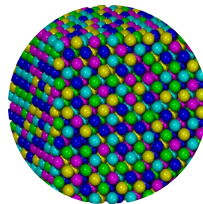
fcc
(Cu, Ni^[4])



Binary Alloys
(Ni-Mo^[4])



Ionic Crystals
(Li₃N^[5])



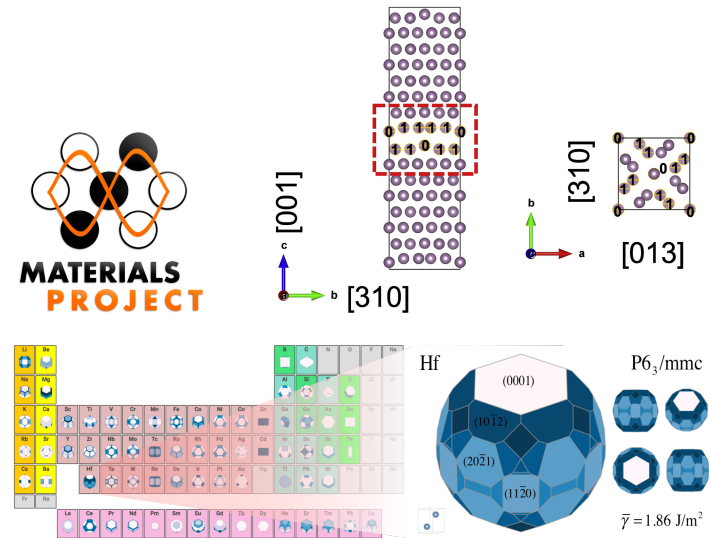
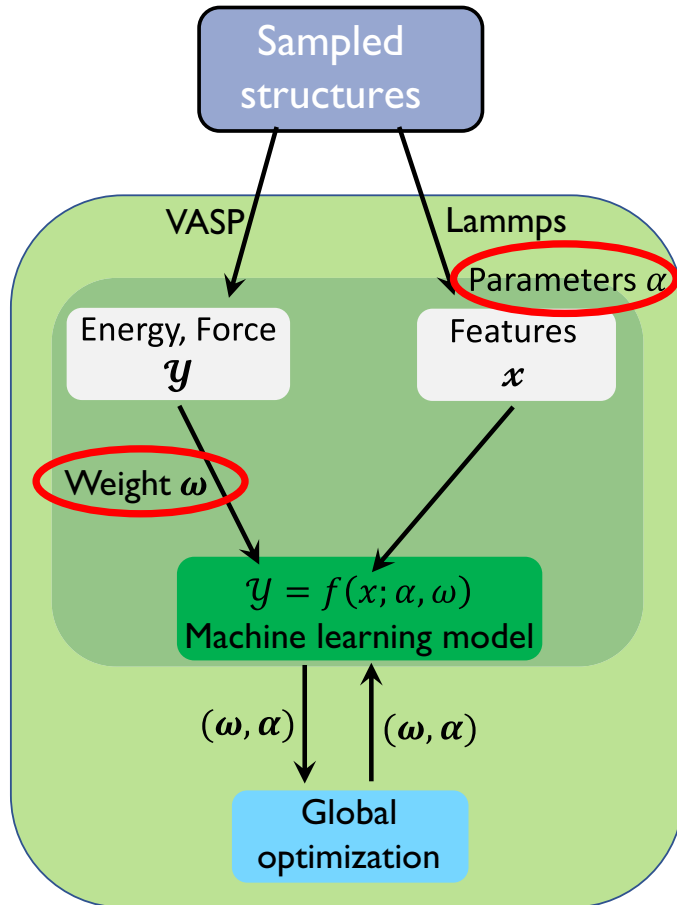
MPE Alloys
(Ta-Nb-Mo-W)

- [1] Thompson et al. *J. Comput. Phys.* **2015**, 285, 316–330.
[2] Wood et al. *arXiv preprint*. **2017**, *arXiv:1702.07042*.
[3] Chen et al. *Phys. Rev. Mater.* **2017**, 1, 043603.

- [4] Li et al. *Phys. Rev. B.* **2018**, 98, 094104.
[5] Deng et al. *npj Comp Mat.* **2019**, 5, 75



Optimization unit

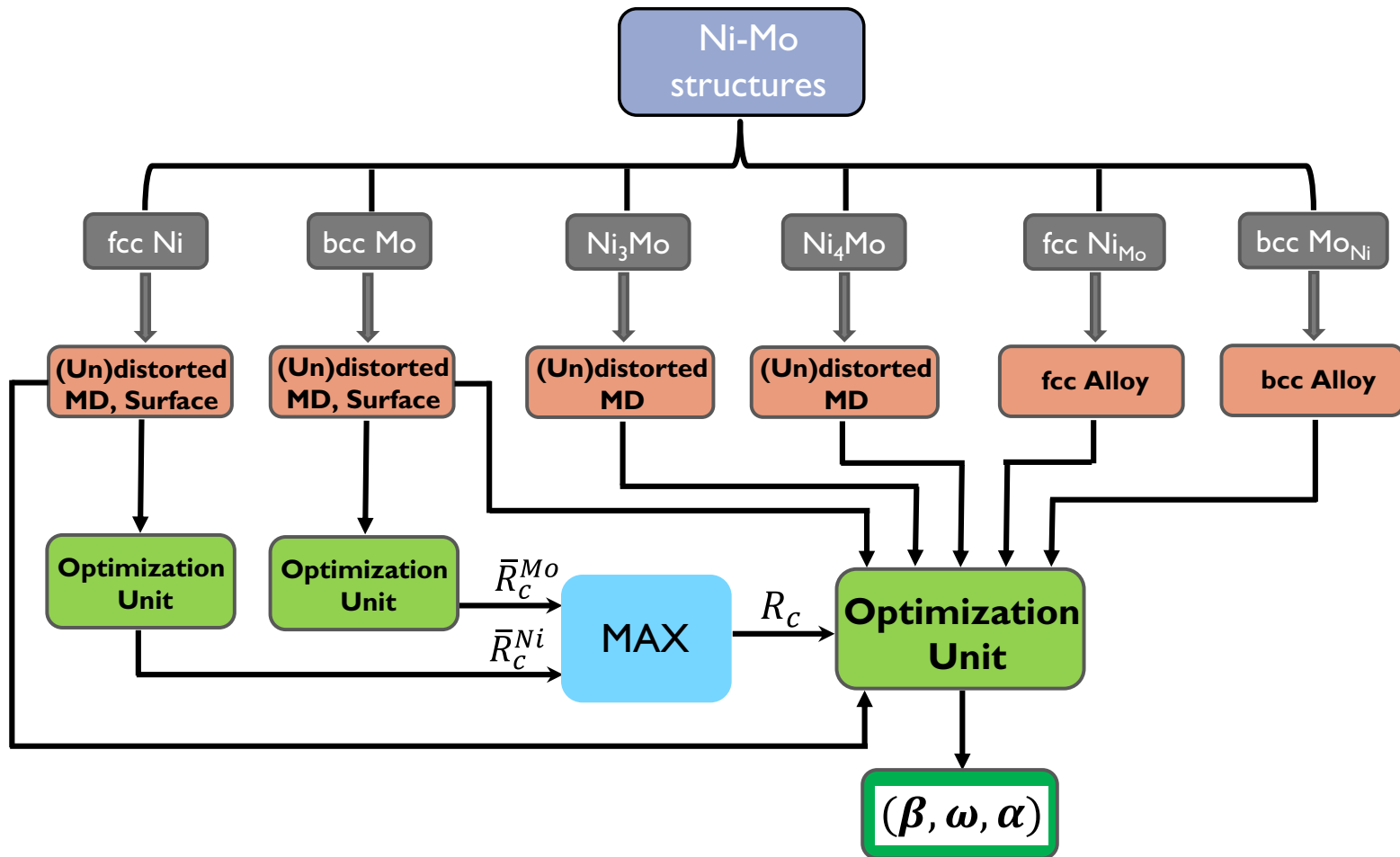


- ¹ Tran et al. Acta Mater. 2016, 117, 91–99 DOI: 10.1016/j.actamat.2016.07.005.
- ² Tran et al. Sci. Data 2016, 3, 160080 DOI: 10.1038/sdata.2016.80.
- ³ Jain, A.; Ong, S. P.; et al. APL Mater. 2013, 1 (1), 11002 DOI: 10.1063/1.4812323.

$$\alpha = (R_{cut}^{atom}, W^{atom})$$

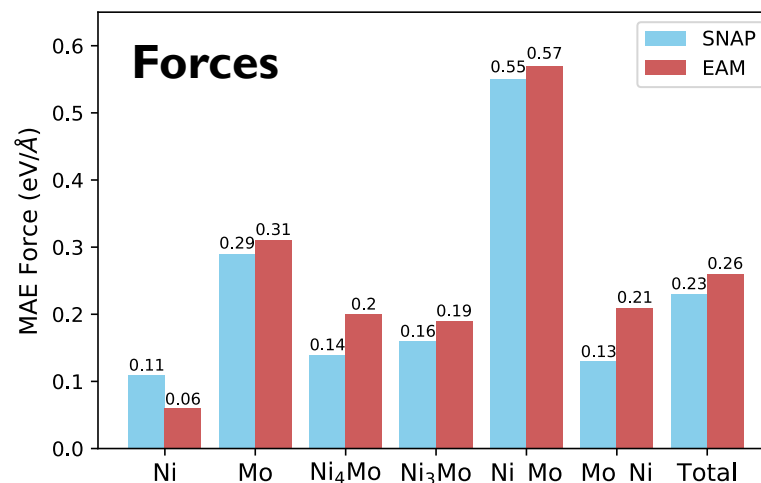
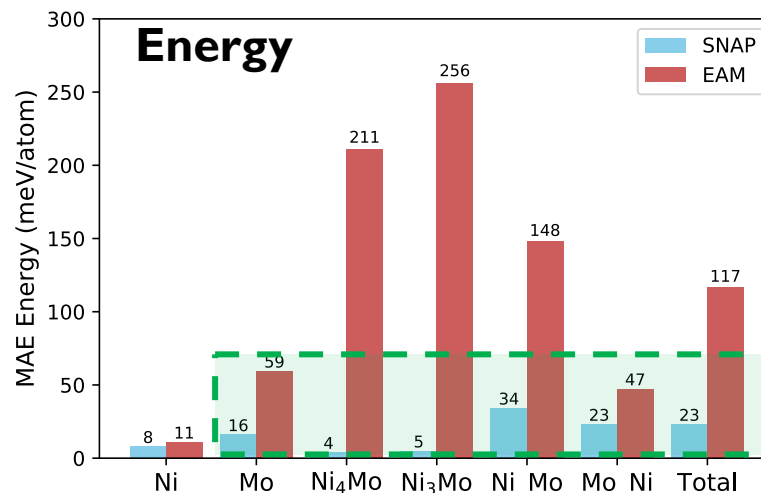
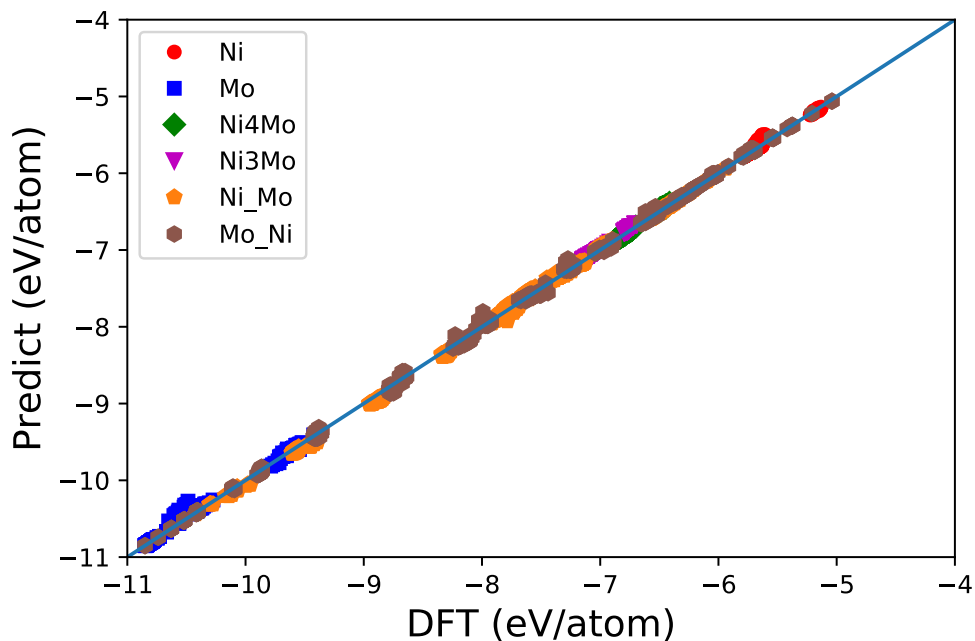
Li, X.; Hu, C.; Chen, C.; Deng, Z.; Luo, J.; Ong, S. P. *Phys. Rev. B*. **2018**, 98, 094104.

Workflow - alloy system



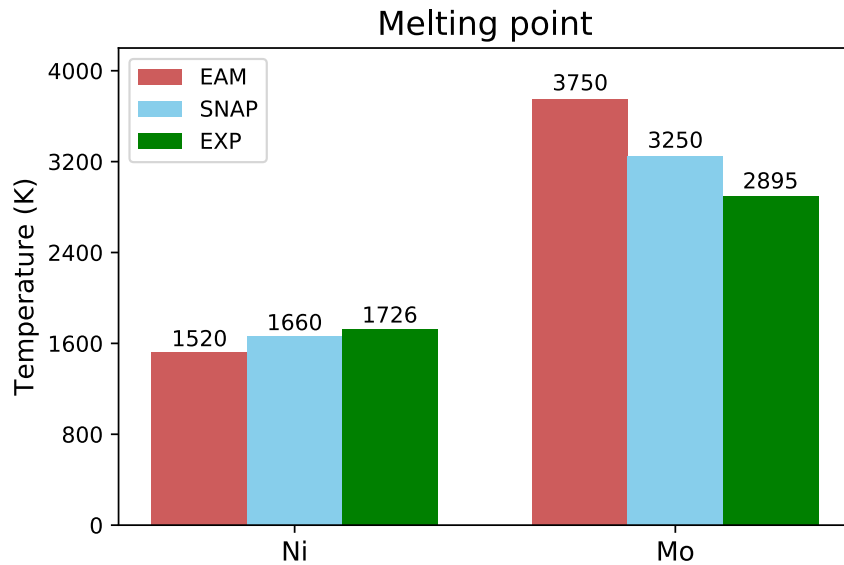
Li, X.; Hu, C.; Chen, C.; Deng, Z.; Luo, J.; Ong, S. P. *Phys. Rev. B*. **2018**, *98*, 094104.

Ni-Mo alloy: SNAP model performance



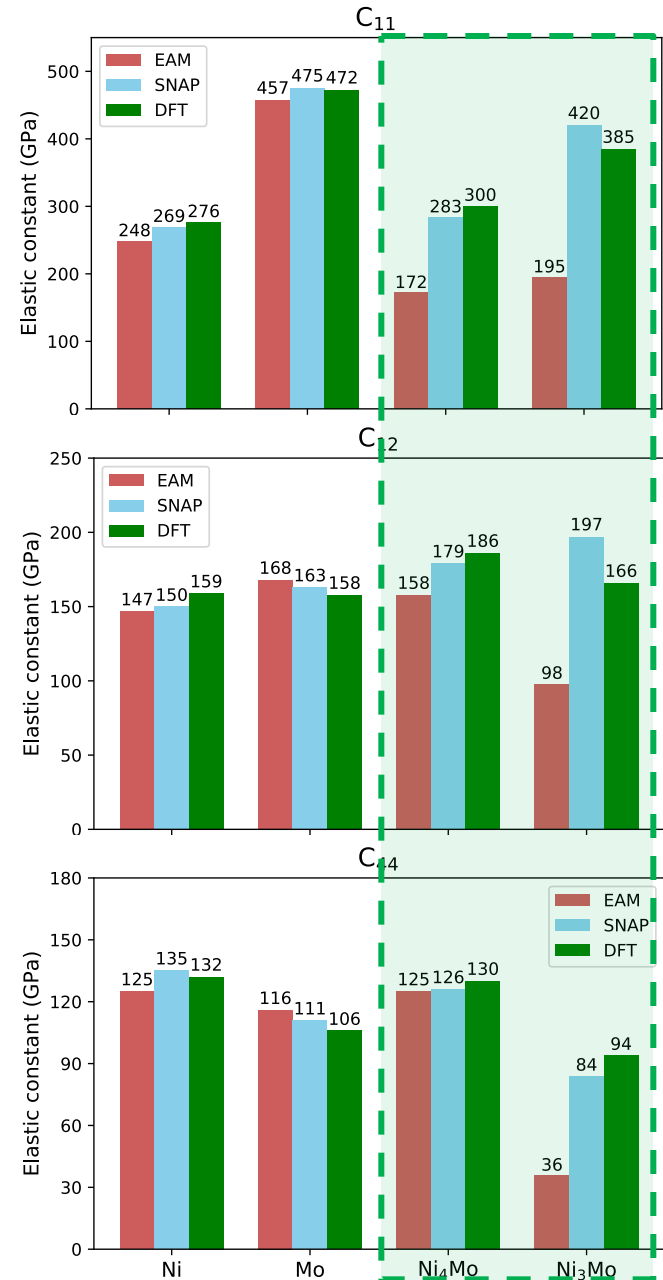
☐ SNAP significantly outperforms in binary and bcc Mo for energy.

Ni-Mo alloy: property matching

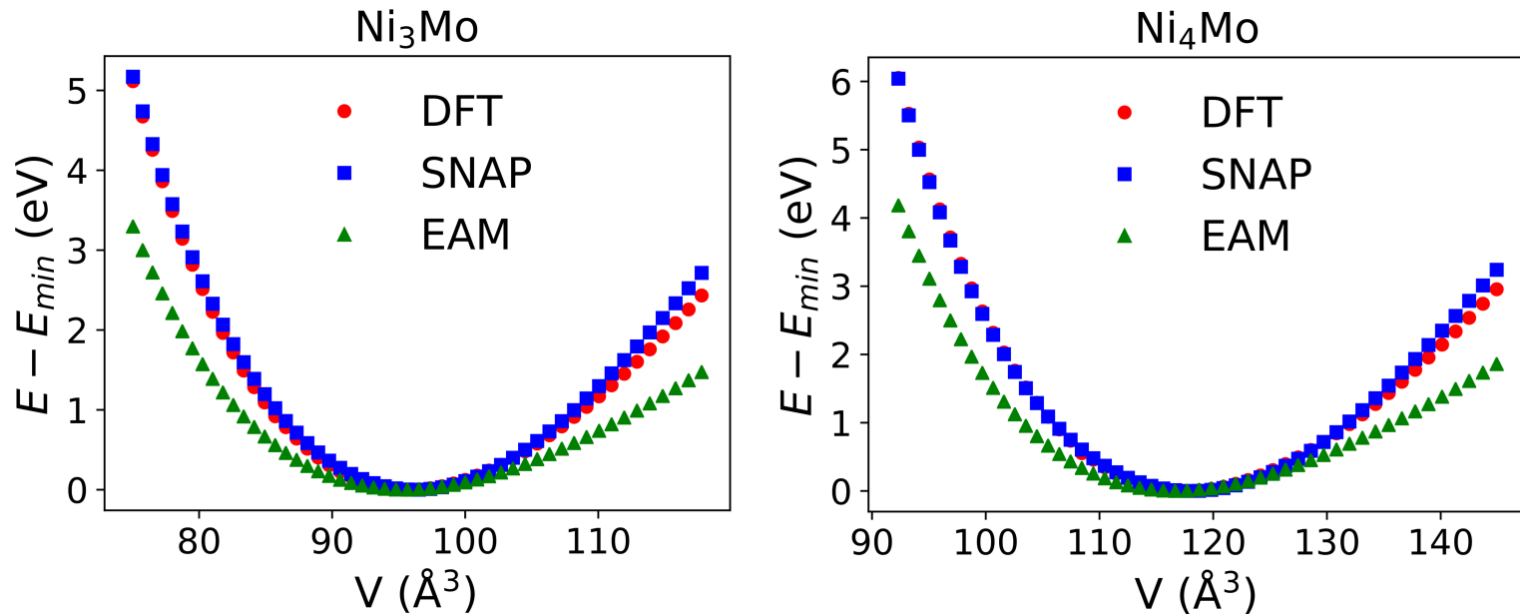


❑ EAM fails in binary bulk systems for elastic constants.

Elastic constants

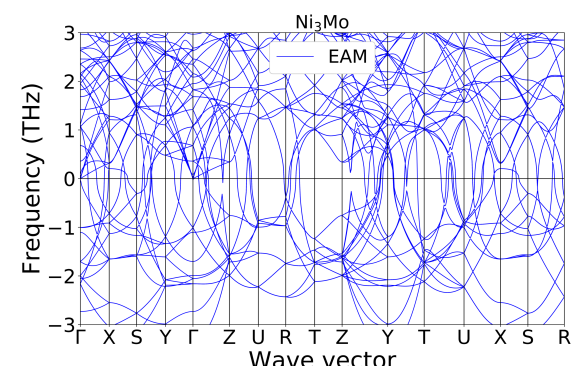
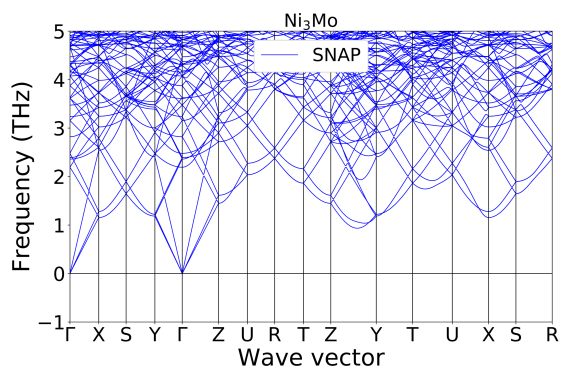
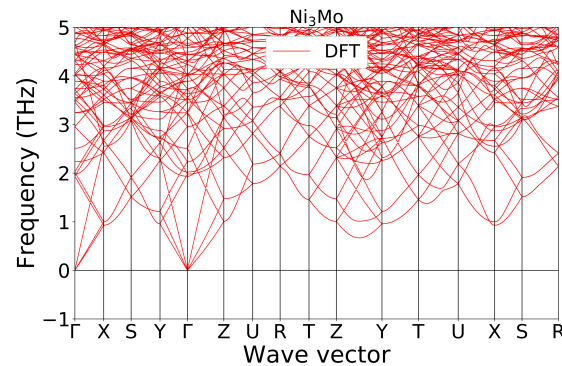
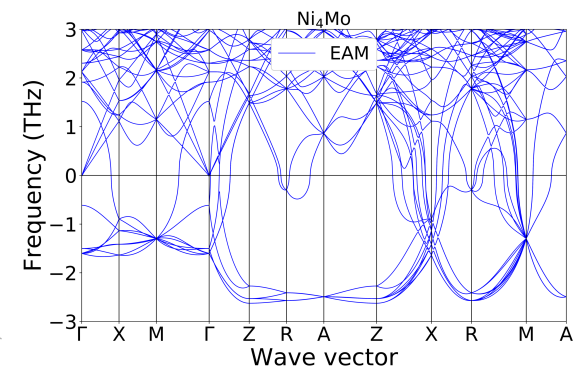
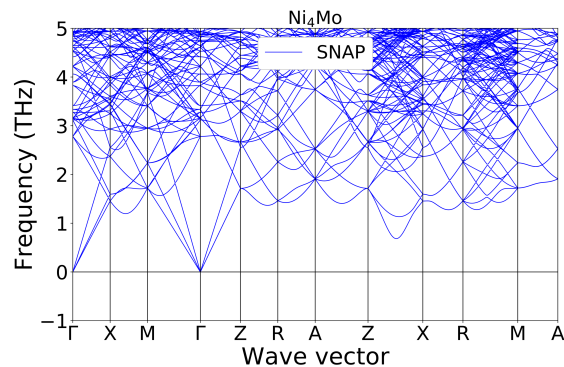
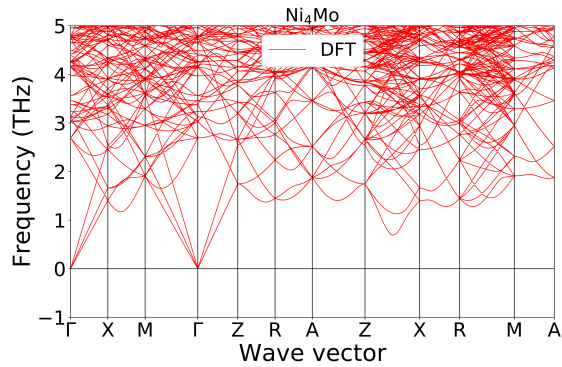


Ni-Mo alloy: Equation of State



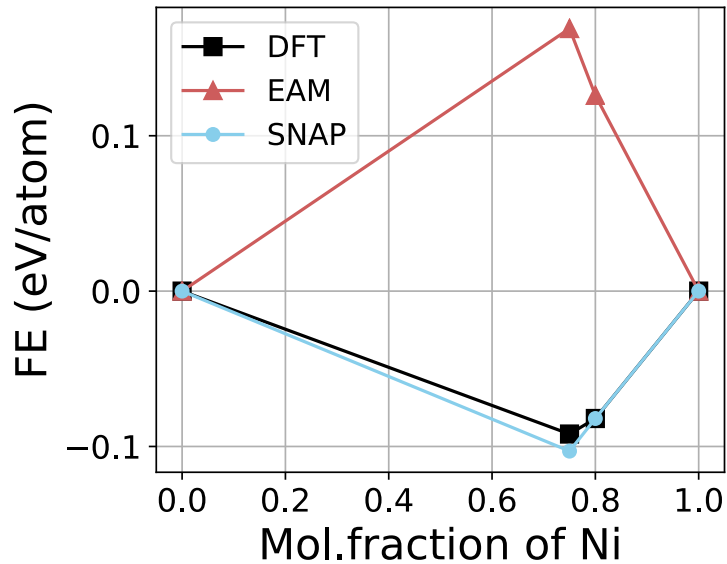
The EAM potential completely fails in the equation of state prediction for binary compounds.

Ni-Mo alloy: Phonon Spectra



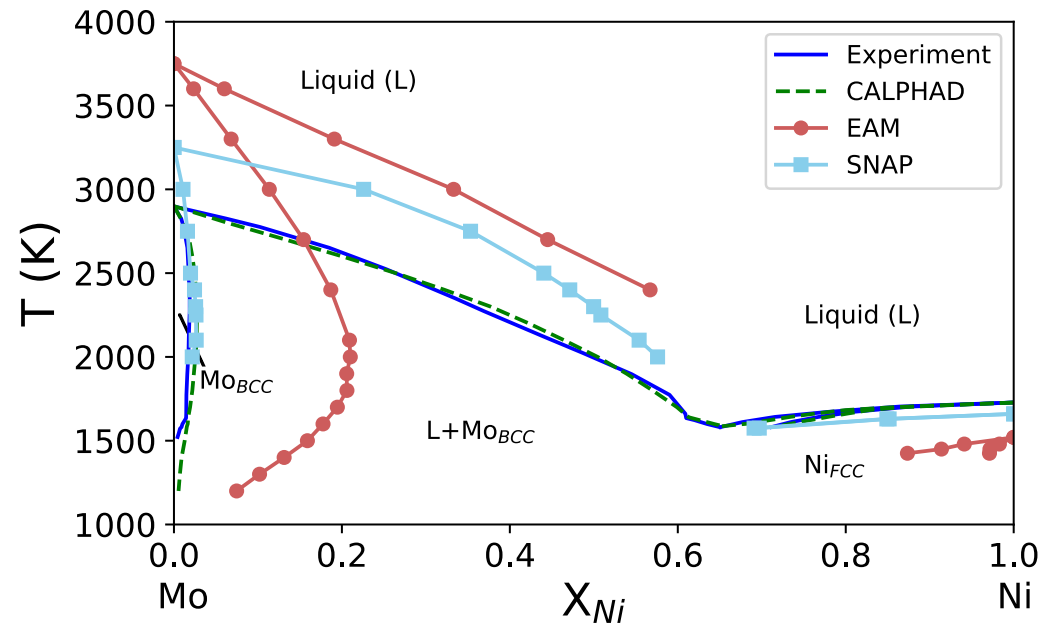
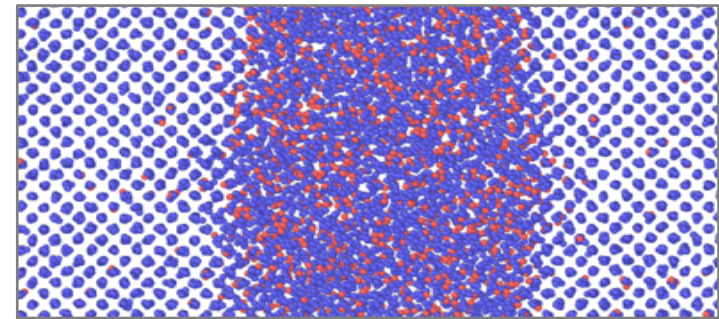
The EAM potential completely fails in the phonon spectra prediction for binary compounds.

Ni-Mo phase diagram

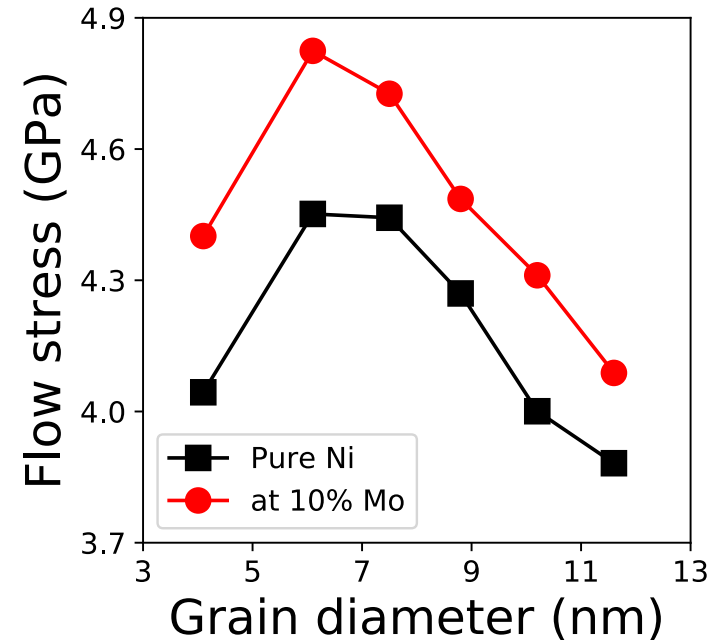
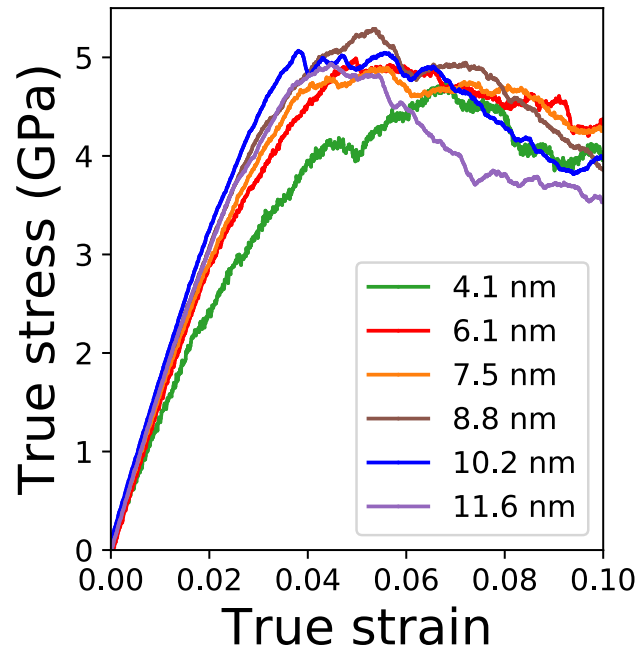


EAM completely fails to reproduce Ni-Mo phase diagram

Solid-liquid equilibrium

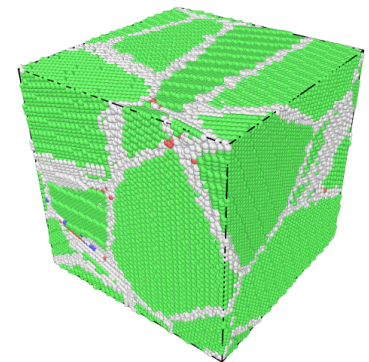


Application: Investigating Hall-Petch strengthening in Ni-Mo

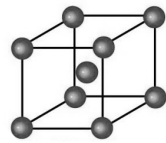


- ❑ ~20,000 to ~455,000 atoms
- ❑ Uniaxially strained with a strain rate of $5 \times 10^8 \text{ s}^{-1}$
- ❑ SNAP reproduces the (inverse) Hall-Petch relationship, consistent with experiment^[1].

[1] Hu et al. *Nature*, 2017, 355, 1292

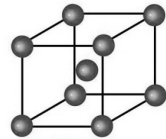


Extending the SNAP formalism



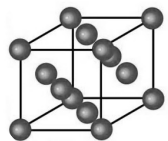
bcc
(Ta^[1], W^[2])

Sandia National Lab

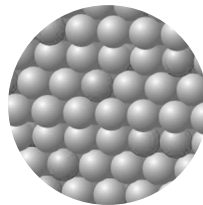


bcc
(Mo^[3])

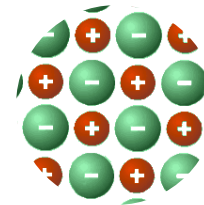
Materials Virtual Lab



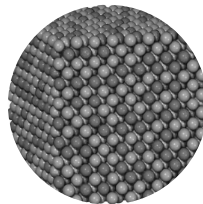
fcc
(Cu, Ni^[4])



Binary Alloys
(Ni-Mo^[4])



Ionic Crystals
(Li₃N^[5])



MPE Alloys
(Ta-Nb-Mo-W)

- [1] Thompson et al. *J. Comput. Phys.* **2015**, 285, 316–330.
[2] Wood et al. *arXiv preprint*. **2017**, *arXiv:1702.07042*.
[3] Chen et al. *Phys. Rev. Mater.* **2017**, 1, 043603.

- [4] Li et al. *Phys. Rev. B.* **2018**, 98, 094104.
[5] Deng et al. *npj Comp Mat.* **2019**, 5, 75

Electrostatic SNAP (eSNAP) for ionic systems

□ Local environment

$$E_{\text{SNAP}} = \beta_0 N + \beta \sum_{i=1}^N B_i$$

□ Electrostatic interaction

$$E_{el} = \frac{q_j q_k}{r}$$

- Formal charge
- Ewald summation

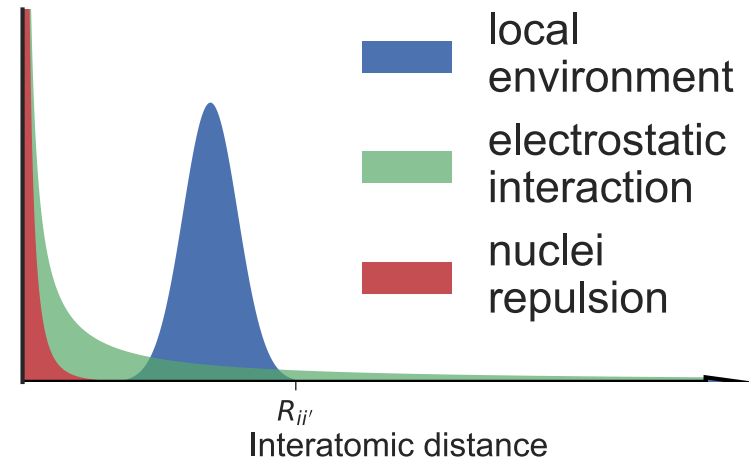
□ eSNAP

$$E_p = \gamma E_{el} + E_{\text{SNAP}}$$

γ - screening parameter

$$\mathbf{F}_j = -\nabla_j E_p = -\gamma \nabla_j E_{el} - F_{j,\text{SNAP}}$$

□ Nuclear repulsion - Ziegler-Biersack-Littmark (ZBL)

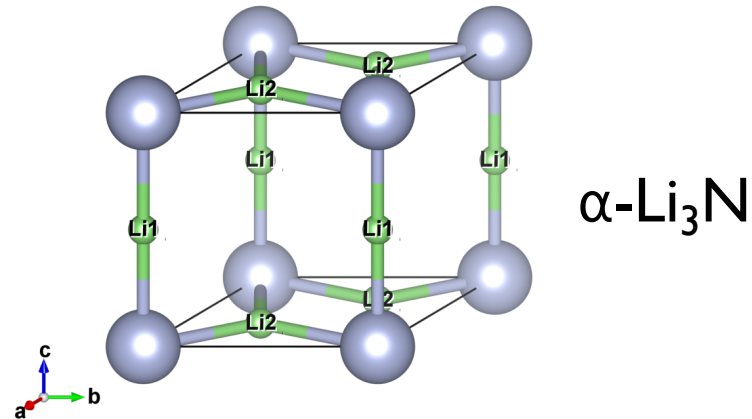


Generation of training data for Li₃N

Initial configuration pool

- ❑ Unit cells with different lattice constant a and c
- ❑ Unit cells with lattice distortions under different strains
- ❑ Snapshots (3x3x3 supercells) taken from AIMD simulated below $1.2T_m$ (400 ~ 1200 K)

Static DFT to calculate reference energy and force

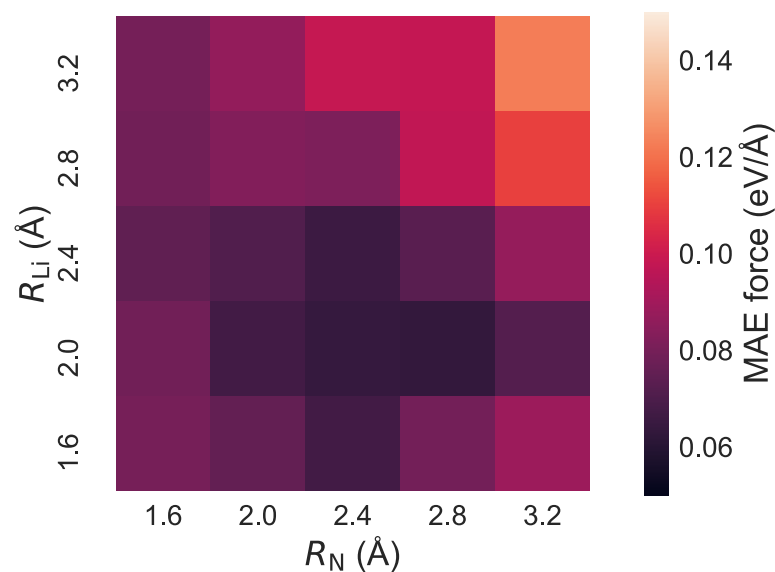
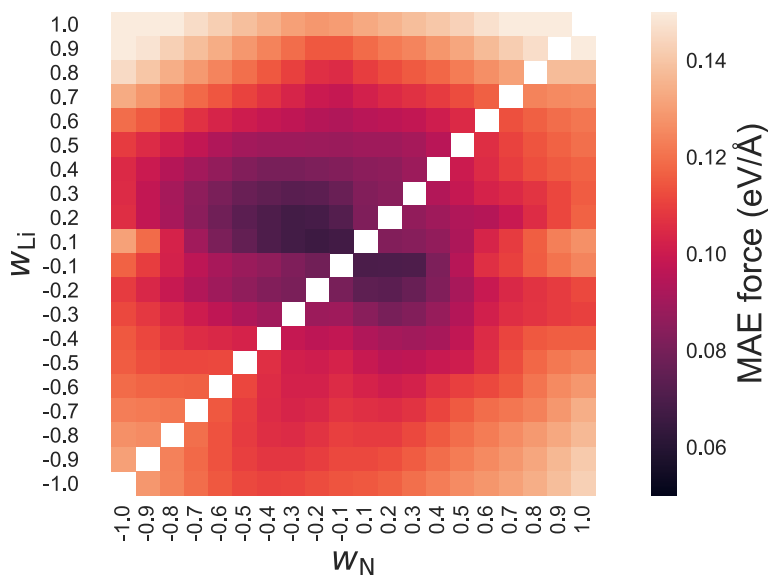


	Distorted unit cells	AIMD snapshots
N_{atoms}	4	108
N_{configs}	109	1000
W_E	10^3	1
W_F	0	10^{-3}

Grid search for hyperparameters of SNAP

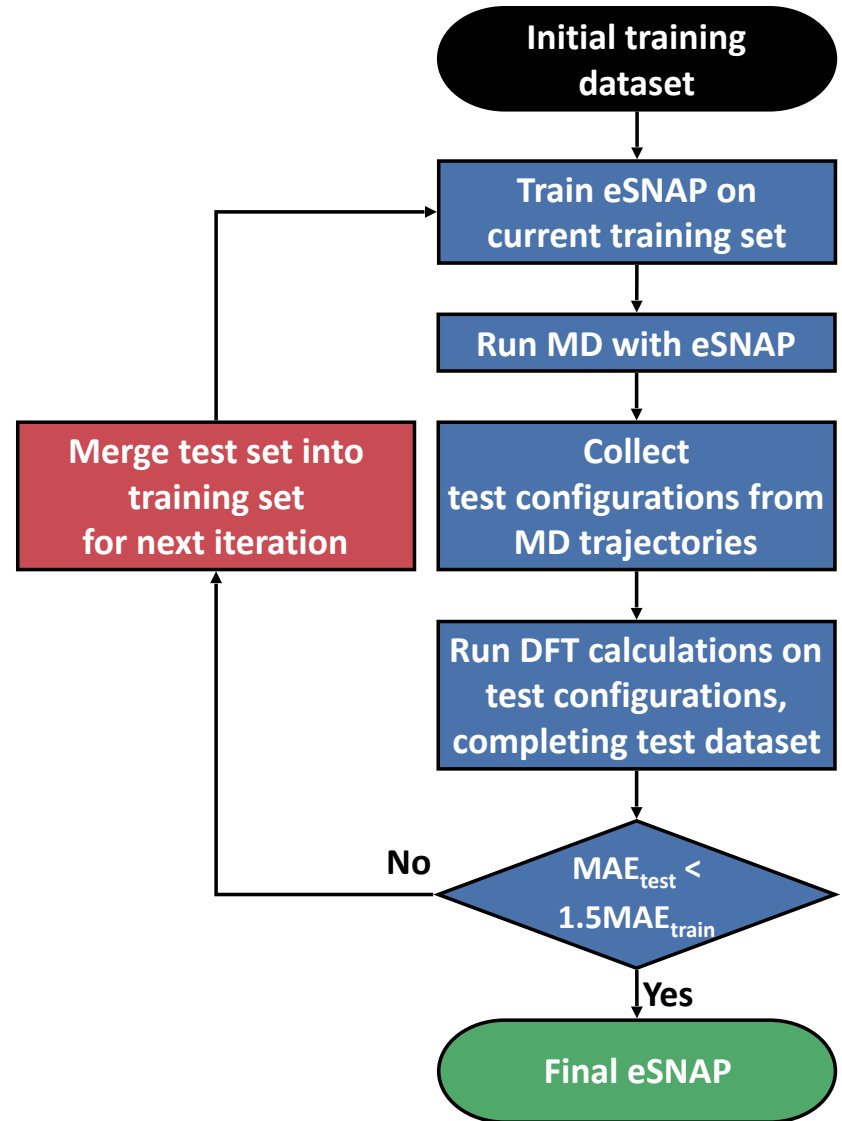
$$\rho_i(\mathbf{r}) = \delta(\mathbf{r}) + \sum_{r_{ii'} < R_{ii'}} f_c(r_{ii'}) w_{ii'} \delta(\mathbf{r} - \mathbf{r}_{ii'})$$

	w	R (Å)
Li	0.1	2.0
N	-0.1	2.8



Training/test iteration

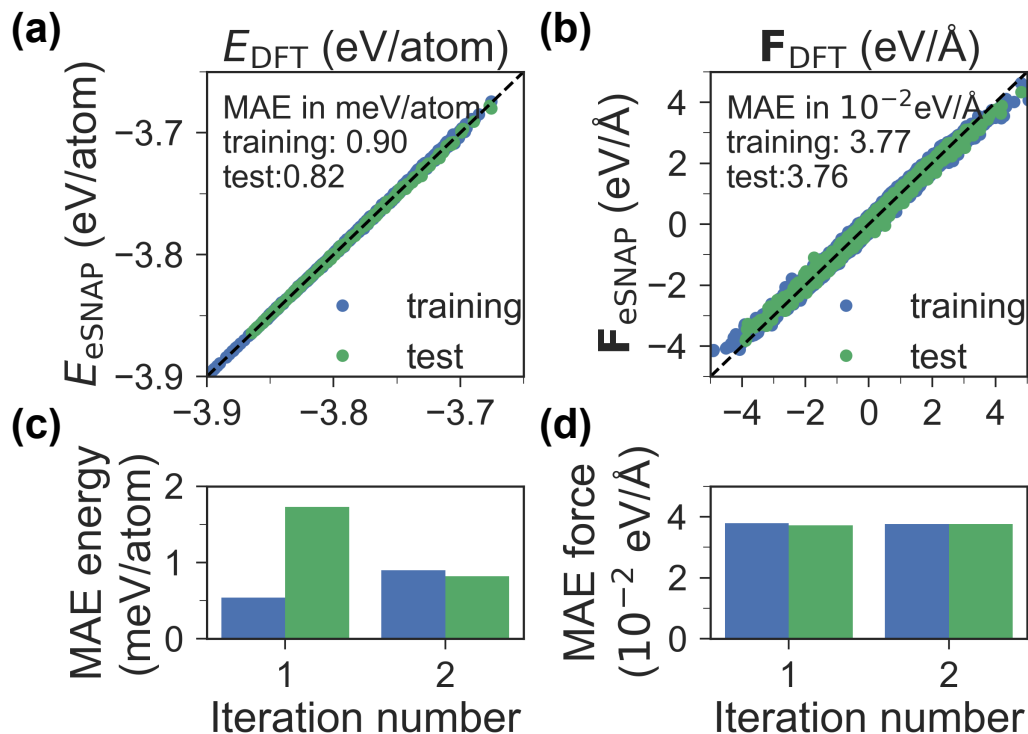
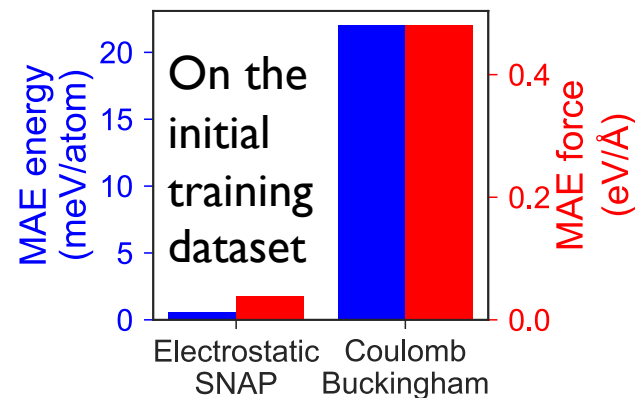
- ❑ Systematically improves the predictions on energy and force for MD simulations
- ❑ Leverages the benefit gained by adding more training instances and the associated costs for performing more DFT calculations



Energy and force prediction from eSNAP

- The iteration terminates with the training data expanded for once.
- eSNAP model has successfully captured the fundamental relationship between atomic environment and energy/force.

Coulomb-Buckingham:
Walker et al. *Philos. Mag. A*
1981, 43 (2), 265–272.



Structural property calculations using eSNAP

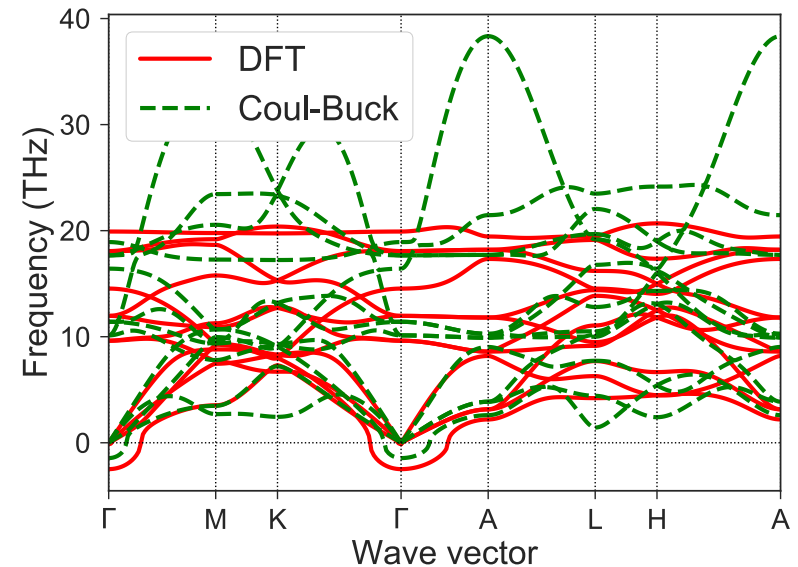
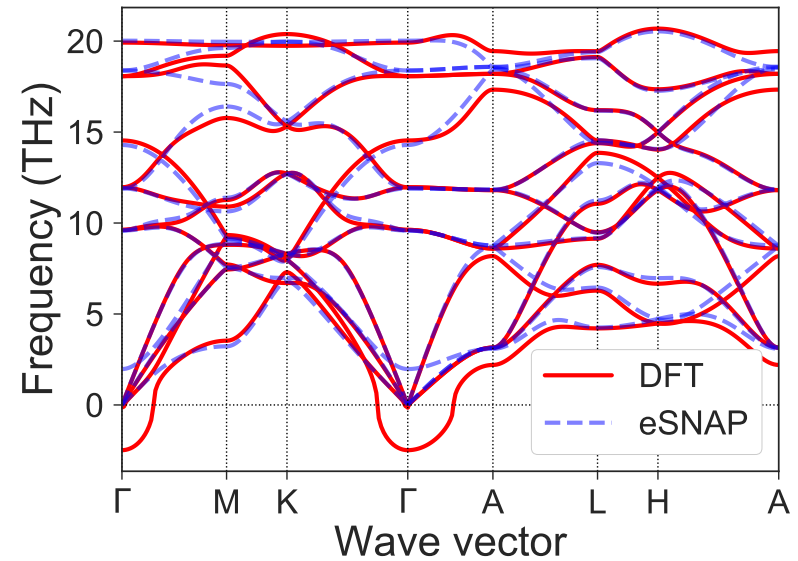
	DFT	eSNAP	Coul-Buck	Exp.
a (Å)	3.641	3.641	3.528	3.648
c (Å)	3.874	3.872	3.628	3.875
c_{11} (GPa)	123	116	165	114
c_{33} (GPa)	137	144	193	118
c_{44} (GPa)	17	17	19	17
c_{66} (GPa)	48	39	53	38
$E_{f,v2}$ (eV)	0.60	0.64	0.44	
$E_{f,v1}$ (eV)	0.51	0.63	0.46	

Coul-Buck: Walker et al. *Philos. Mag. A* **1981**, 43 (2), 265–272.

Exp:

Rabenau et al. *J. Less-Common Met.* **1976**, 50 (1), 155–159.

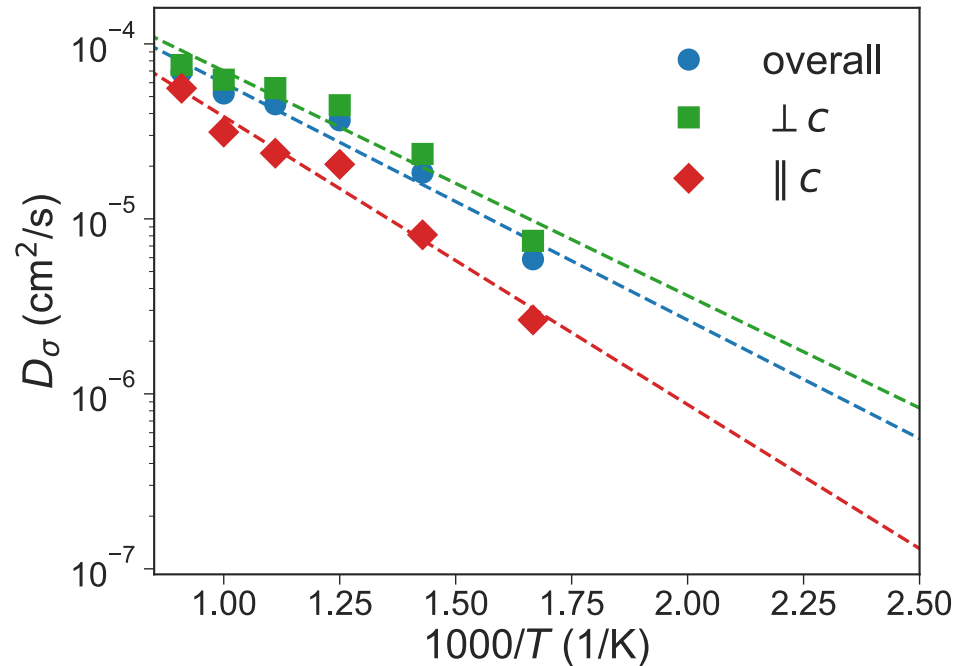
Kress et al. *Phys. Rev. B* **1980**, 22 (10), 4620–4625.



Deng et al. *npj Comp Mat.* **2019**, 5, 75

Bulk diffusion

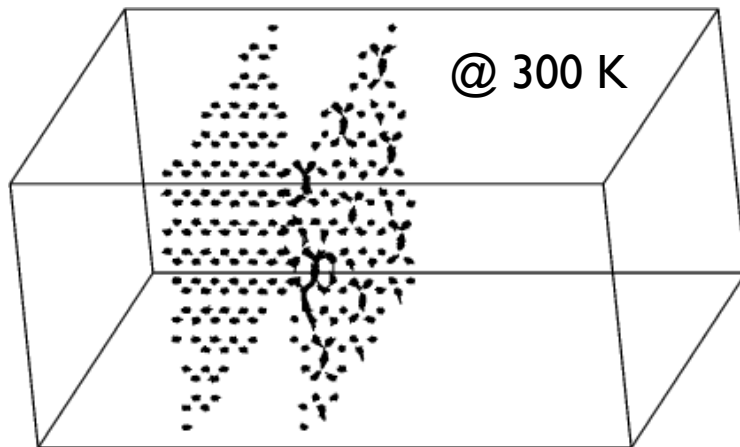
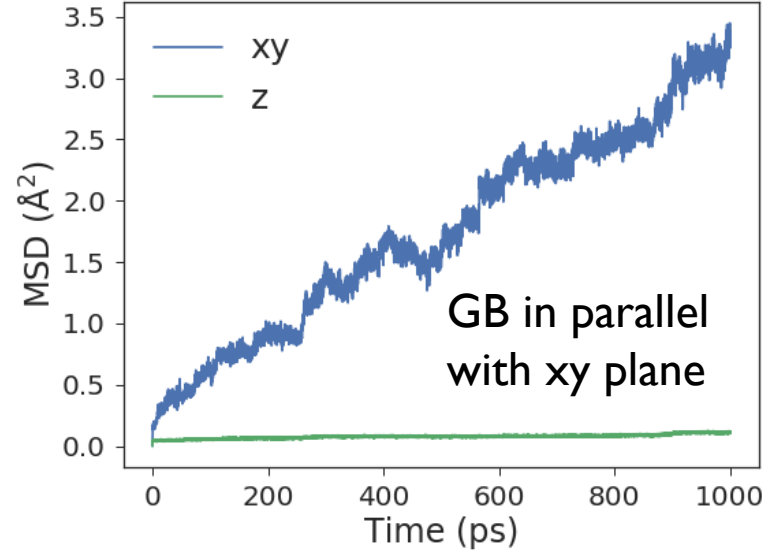
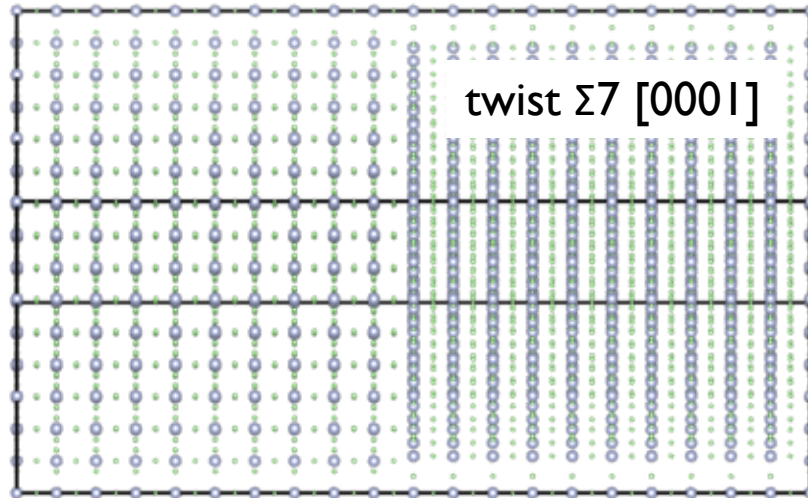
- Simulation box contains 4000 atoms (10x10x10 supercell)
- MD simulations performed from 600 to 1000 K in an *NVT* ensemble for Ins



	E_a (eV)			σ_{RT} (mS/cm)		
	ab	c	total	ab	c	total
eSNAP	0.255	0.327	0.269	29.6	2.32	17.3
Exp.	0.290	0.490		1.20	0.01	

Exp.: Alpen et al. *Appl. Phys. Lett.*
1977, 30 (12), 621–623.

Grain boundary diffusion



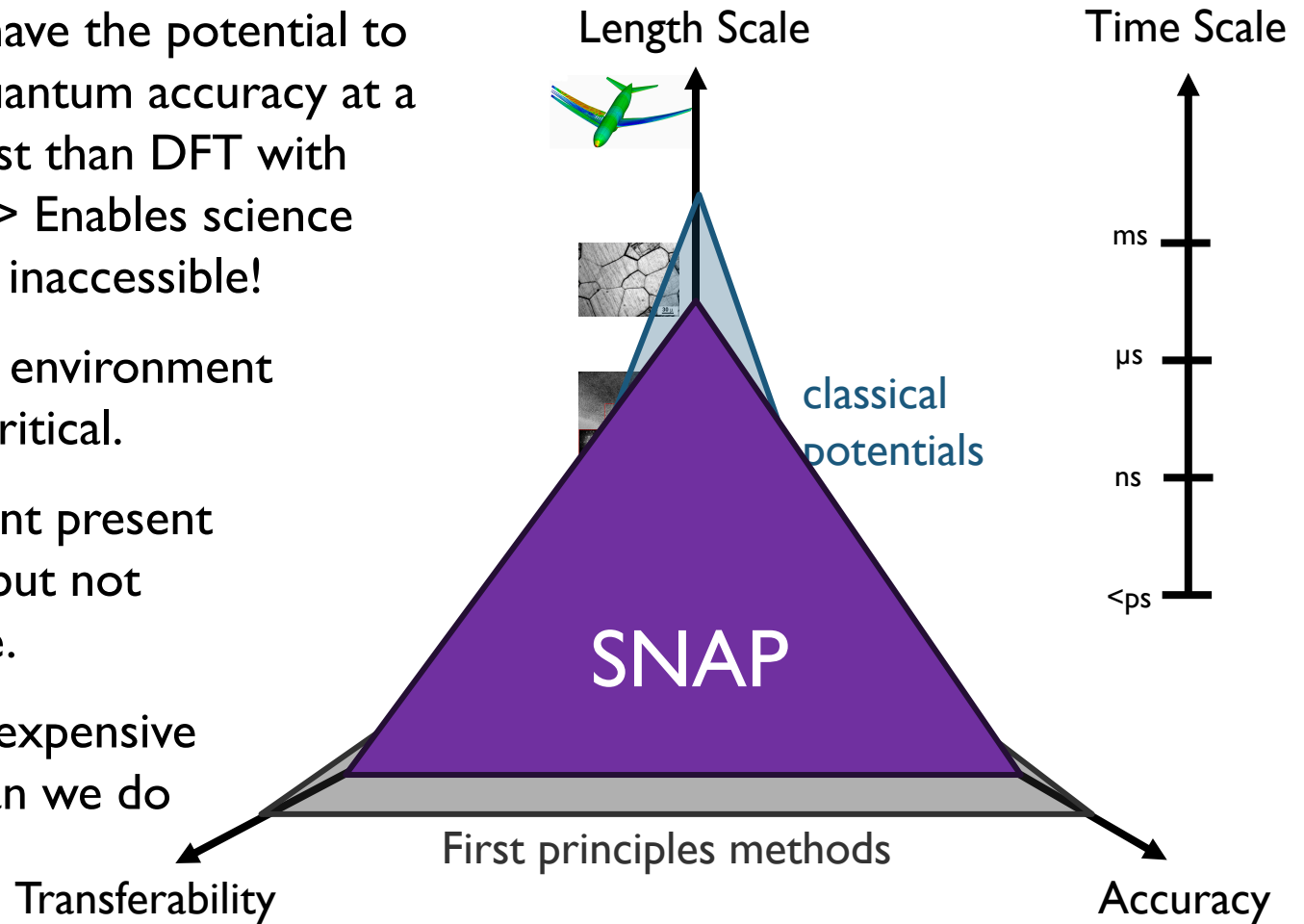
The presence of GB facilitates Li diffusion

D^* at 300 K

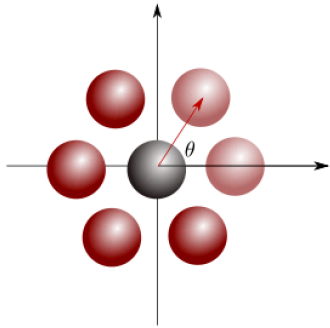
- GB: $7.09 \times 10^{-8} \text{ cm}^2/\text{s}$
- Bulk (extrapolated): $2.24 \times 10^{-8} \text{ cm}^2/\text{s}$

Conclusions

- ✓ ML potentials have the potential to achieve near-quantum accuracy at a much lower cost than DFT with linear scaling => Enables science that is hitherto inaccessible!
- ✓ Choice of local environment description is critical.
- ✓ Multi-component present complications, but not insurmountable.
- X 10-100x more expensive than MEAM (can we do better?)



Machine learning the potential energy surface



$$G_i^{\text{atom,rad}} = \sum_{j \neq i}^{N_{\text{atom}}} e^{-\eta(R_{ij}-R_s)^2} \cdot f_c(R_{ij}),$$

ACSF/MTP encodes atomic distances and angles.

$$G_i^{\text{atom,ang}} = 2^{1-\zeta} \sum_{j,k \neq i}^{N_{\text{atom}}} (1 + \lambda \cos \theta_{ijk})^\zeta \cdot e^{-\eta'(R_{ij}^2+R_{ik}^2+R_{jk}^2)} \cdot f_c(R_{ij}) \cdot f_c(R_{ik}) \cdot f_c(R_{jk}),$$

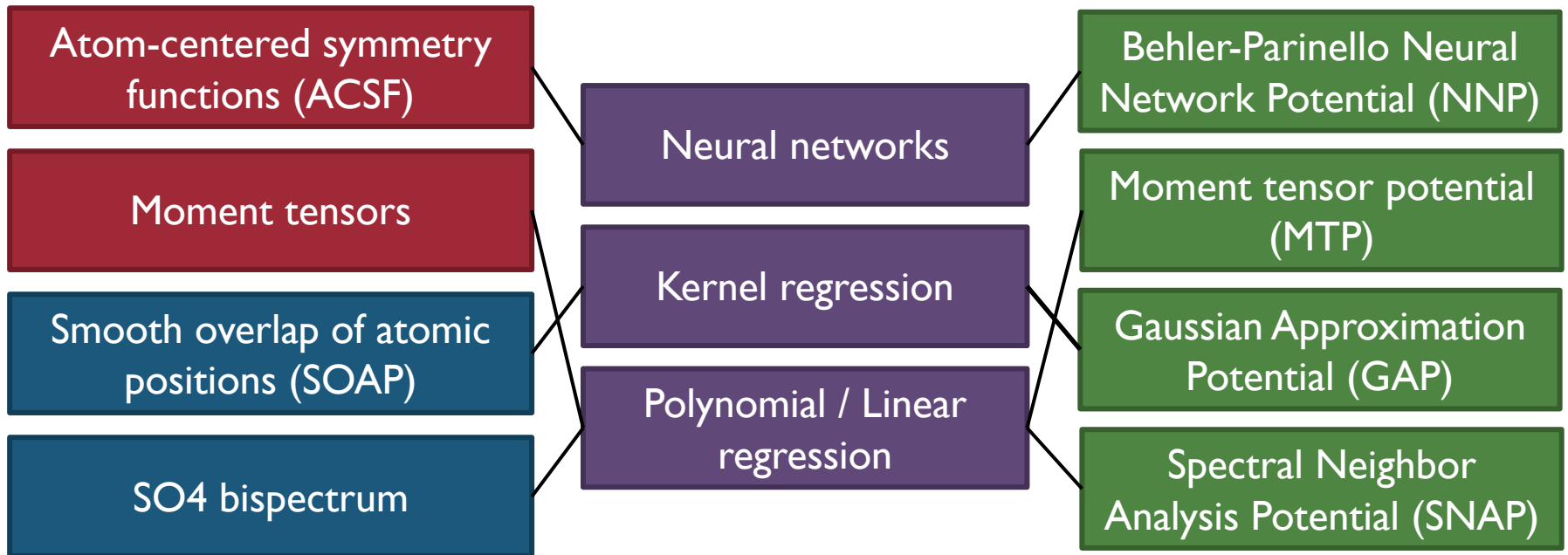
$$\rho_i(\mathbf{R}) = \sum_j f_c(R_{ij}) \cdot \exp\left(-\frac{|\mathbf{R} - \mathbf{R}_{ij}|^2}{2\sigma_{\text{atom}}^2}\right)$$

SOAP/bispectrum encodes atomic neighbor density.

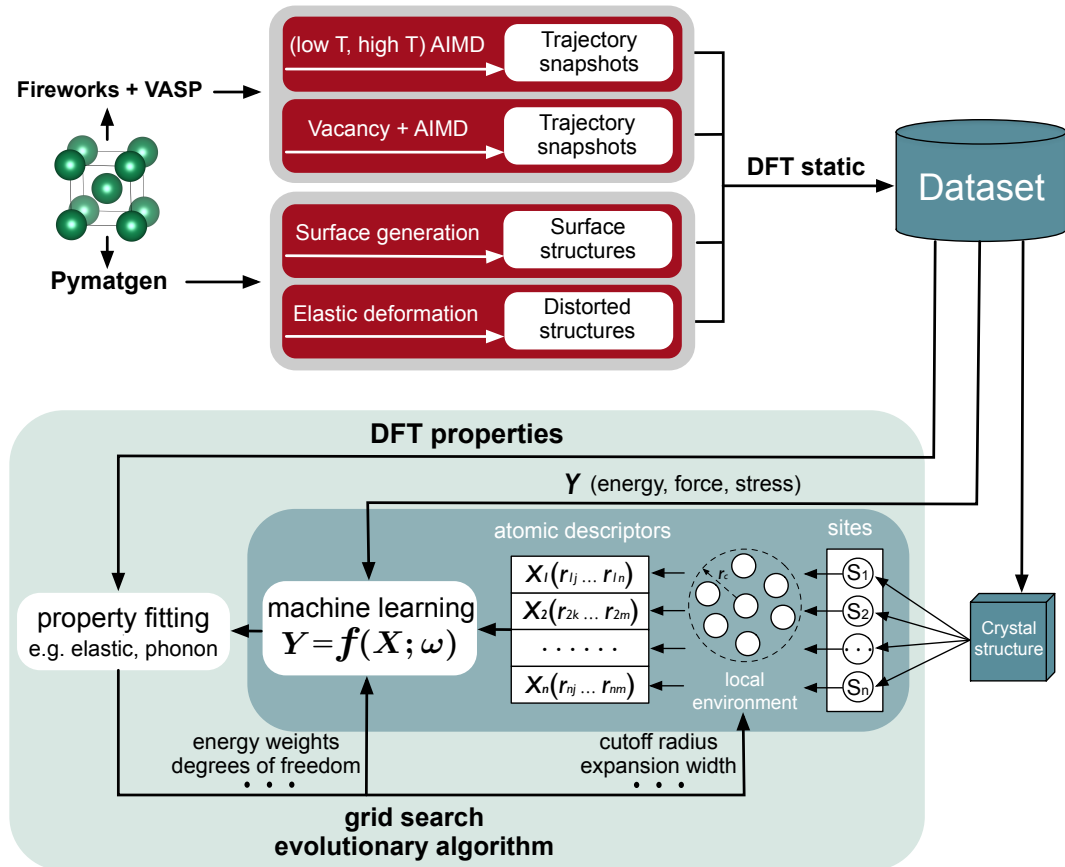
Local environment descriptors

ML approach

Interatomic Potential



Standardized workflow for ML-IAP construction and evaluation



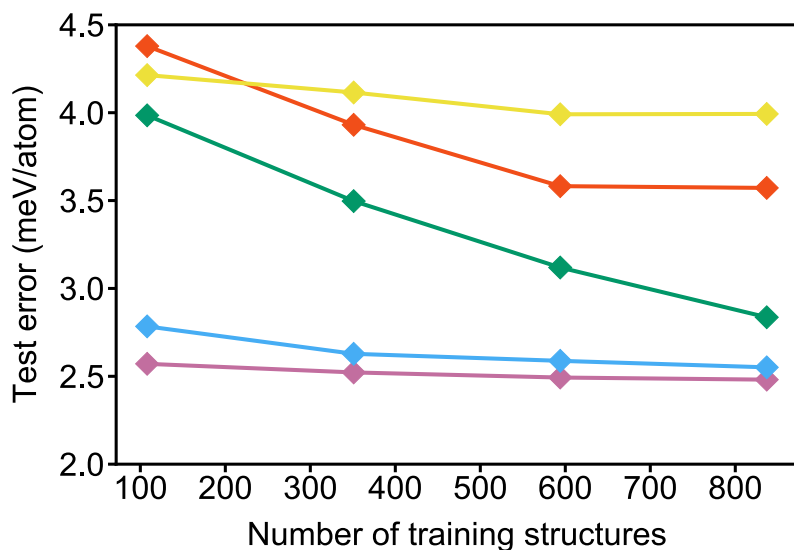
Test systems:

- Fcc Ni
- Fcc Cu
- Bcc Li
- Bcc Mo
- Diamond Ge
- Diamond Si

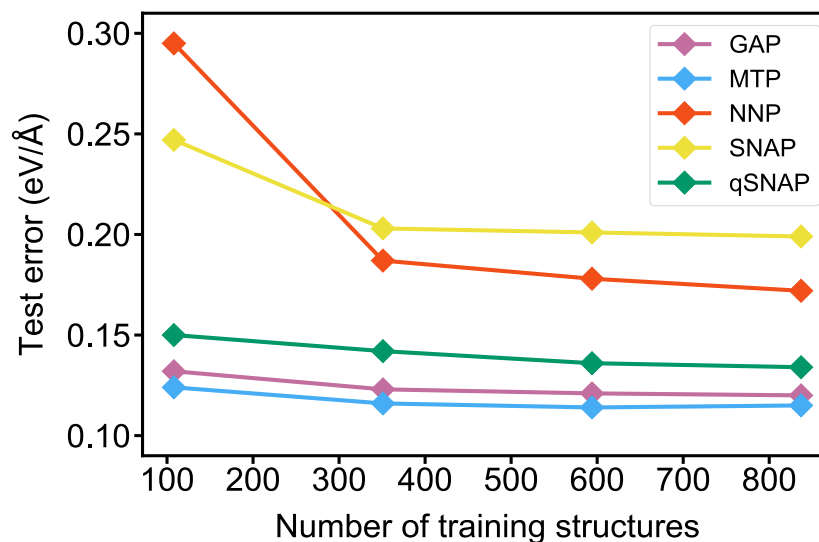
Available open source on Github: <https://github.com/materialsvirtuallab/mlearn>

ML-IAP: Training Data Requirements

Energies

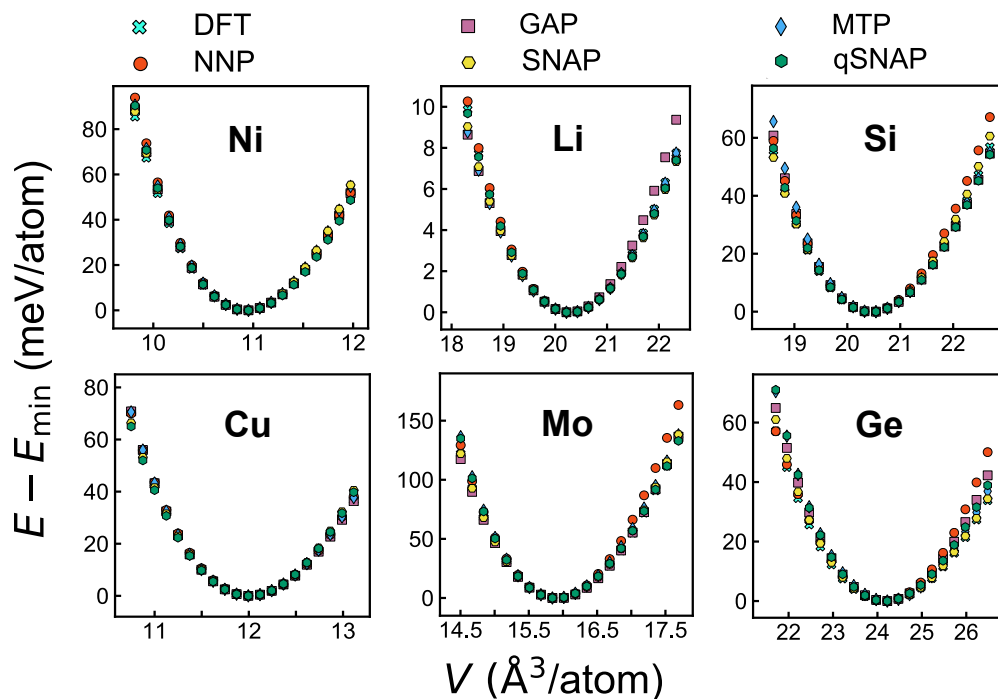


Forces

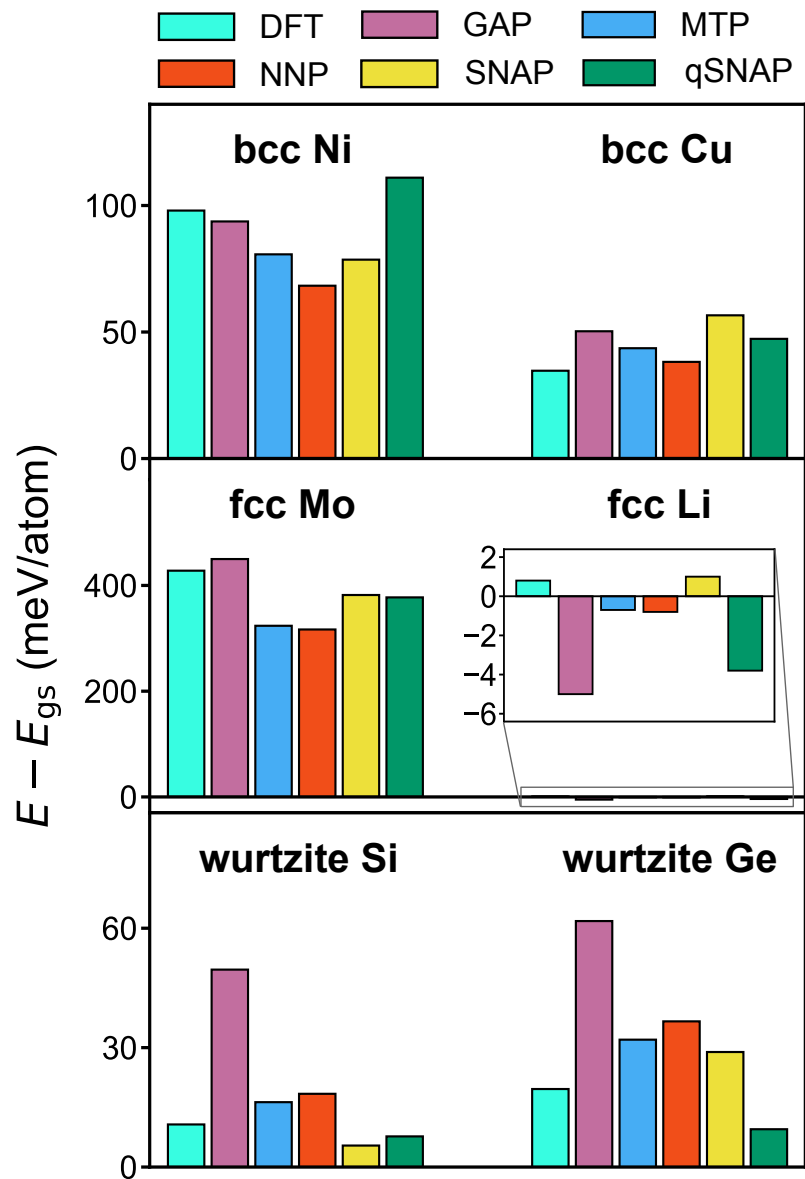


- Data quality is more important than data quantity - $\sim O(100)$ structures sufficient to converge
- NNP and qSNAP require much more training data than other models.

ML-IAP: Extrapolability



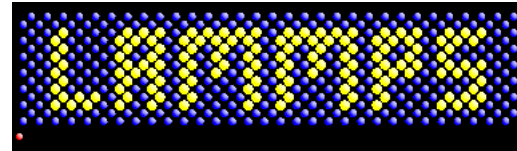
- The greater the ML complexity (e.g., NNP and GAP), the greater the issues with extrapolation.
- Linear SNAP performs surprisingly well on EOS and polymorph energy differences.



Acknowledgements

- **Shyue Ping Ong**
- Zhi Deng
- Yunxing Zuo
- Chi Chen

Where to get the potentials?



<https://github.com/materialsvirtuallab/snap>

- Xiang-Guo Li. *et al.* *Phys. Rev. B*, 98, 094104 (2018)
- Zhi Deng. *et al.* *npj Comp Mat*, 5, 75 (2019)
- Yunxing Zuo, *et al.* “A Performance and Cost Assessment of Machine Learning Interatomic Potentials”, arXiv:1906.08888 (2019)



XSEDE

Extreme Science and Engineering
Discovery Environment

